THE JOURNAL OF BIOLOGICAL CHEMISTRY
Vol. 274, No. 29, Issue of July 16, pp. 20473–20478, 1999

Printed in U.S.A.

Solution Structure of the Major α-Amylase Inhibitor of the Crop Plant Amaranth*

(Received for publication, February 18, 1999, and in revised form, April 14, 1999)

Shanyun Lu‡, Pengchi Deng‡, Xiucai Liu§, Jingchu Luo‡, Rushan Han‡, Xiaocheng Gu‡¶, Songping Liang‖, Xianchun Wang‖, Feng Li‖, Valentin Lozanov, András Patthy§§, and Sándor Pongor**¶¶**

*From the ‡Peking University, Beijing 100871, China, §Cathay Biotech Company, Beijing 10080, China, ‖Hunan Normal University, Hunan, China, **International Centre for Genetic Engineering and Biotechnology, Trieste 34012, Italy, §§Agricultural Biotechnology Centre, Gödöllö, 2102, Hungary*

α-Amylase inhibitor (AAI), a 32-residue miniprotein from the Mexican crop plant amaranth (*Amaranthus hypochondriacus*), is the smallest known α-amylase inhibitor and is specific for insect α-amylases (Chagolla-Lopez, A., Blanco-Labra, A., Patthy, A., Sanchez, R., and Pongor, S. (1994) *J. Biol. Chem.* 269, 23675–23680). Its disulfide topology was confirmed by Edman degradation, and its three-dimensional solution structure was determined by two-dimensional ^{1}H NMR spectroscopy at 500 MHz. Structural constraints (consisting of 348 nuclear Overhauser effect interproton distances, 8 backbone dihedral constraints, and 9 disulfide distance constraints) were used as an input to the X-PLOR program for simulated annealing and energy minimization calculations. The final set of 10 structures had a mean pairwise root mean square deviation of 0.32 Å for the backbone atoms and 1.04 Å for all heavy atoms. The structure of AAI consists of a short triple-stranded β-sheet stabilized by three disulfide bonds, forming a typical knottin or inhibitor cystine knot fold found in miniproteins, which binds various macromolecular ligands. When the first intercystine segment of AAI (sequence IPKWNR) was inserted into a homologous position of the spider toxin Huwentoxin I, the resulting chimera showed a significant inhibitory activity, suggesting that this segment takes part in enzyme binding.

Plant seeds produce a large variety of enzyme inhibitors that are thought to provide protection against insects and microbial pathogens. As plant seed inhibitors are often species specific, *i.e.* they inhibit enzymes of a well defined group of pathogenic organisms but do not affect the mammalian counterpart, they make attractive candidates for conferring pest resistance to transgenic plants (for a review see Ref. 1).

The α-amylase inhibitors vary considerably in their structures. Many of their structural relatives, *e.g.* proteinase inhibitors, osmotin, and salt-induced proteins (Table I), play roles in plant stress response. The smallest of the known α-amylase inhibitors, AAI,[1] is found in the seeds of *Amaranthus hypochondriacus*, a variety of the Mexican crop plant amaranth or Prince's feather (2). AAI is a 32-residue polypeptide with three disulfide bridges, which has no significant sequence similarity to other proteins in the data bases. It has a spurious sequence similarity to various members of the so-called knottin (3) or "inhibitor-type cystine knot" (4) family, which includes various proteinase inhibitors and toxins. AAI is species specific; it inhibits α-amylase of several pathogenic insect larvae (*Tribolium castaneum*, *Prostaphanus truncatus, Periplaneta americana,* and *Tenebrio mollitor)* but not the mammalian α-amylases.

Here we report the three-dimensional structure of AAI as determined by NMR spectroscopy and show via amino acid replacement and chimera construction that a short segment of the first loop of AAI is involved in enzyme inhibition.[2]

EXPERIMENTAL PROCEDURES

Materials

AAI was prepared as described (5). Sephadex G-75 and DEAE-Sepharose CL6B were obtained from Amersham Pharmacia Biotech. α-Chymotrypsin, endoproteinase Glu-C, and trypsin were obtained from Sigma; cyanogen bromide and vinyl pyridine were obtained from Aldrich. All chemicals used were of analytical or sequencing grade. HPLC grade acetonitrile and trifluoroacetic acid were obtained from Aldrich.

Assay of α-Amylase Inhibition

Crude α-amylase from *T. mollitor* and *P. americana* larvae was extracted and partially purified as described (6). Assays of α-amylase inhibition were performed according to Bernfeld (7) as described (5).

Peptide Mapping and N-terminal Sequencing

A 75-μg sample of AAI was dissolved in 150 μl of 0.2 M Tris-HCl buffer, pH 7.3, and digested with a mixture of trypsin (3 μg), chymotrypsin (3 μg), and endoproteinase Glu-C (3 μg) at 37 °C for 15 h. The mixture was separated by reverse phase-HPLC on a Vydac C_{18} column (2.1 × 250 mm). Selected peaks were collected, lyophilized, and covalently coupled to aminophenyl glass beads in prepacked capillary

* The work at Peking University was supported by a grant from the Collaborative Research Program of the International Center of Genetic Engineering and Biotechnology (Trieste, Italy) and grants from the National Science Foundation of China and the National High Technology Program of China. The costs of publication of this article were defrayed in part by the payment of page charges. This article must therefore be hereby marked "*advertisement*" in accordance with 18 U.S.C. Section 1734 solely to indicate this fact.

The atomic coordinates and structure factors (code 1qfd) have been deposited in the Protein Data Bank, Brookhaven National Laboratory, Upton, NY.

¶ To whom correspondence may be addressed. Tel./Fax: 86 10 6275 1843; E-mail: guxc@/sc.pku.edu.cn.

¶¶ To whom correspondence may be addressed: International Centre for Genetic Engineering and Biotechnology (ICGEB), Padriciano 99, Trieste 34012 Italy. Tel.: 39 040 3757300; Fax: 39 040 226 555; E-mail: pongor@icgeb.trieste.it.

[1] The abbreviations used are: AAI, α-amylase inhibitor; CB, cellulose-binding domain; COSY, correlation spectroscopy; TOCSY, total correlation spectroscopy; HPLC, high pressure liquid chromatography; FMOC, 9-fluorenylmethyoxycarbonyl; DQF-COSY, double quantum filtered correlation spectroscopy; NOESY, nuclear Overhauser effect spectroscopy.

[2] NMR spectroscopy was determined in the lab of Dr. X. Gu (guxc@lsc.pku.edu.cn). The disulfide structure and the chimera construction were carried out in the lab of Dr. S. Liang (liangsp@public.cs.hn.cn). AAI and its analogs were synthesized in the lab of Dr. S. Pongor (pongor@icgeb.trieste.it).

TABLE I
Structural classification of α-amylase inhibitors
Based on a classification by Richardson (33) and completed with recent data (2). ND, no data.

Class	Source	Size (amino acids)	½Cys	Inhibitory activity			Members of the group with other activities
				Against insect amylases	Against mammalian or other amylases	Against proteases	
Kunitz type	Barley (29), wheat (30), rice (6)	176–180	2–4	+	+	+	Miraculin (32)
Cereal type	Wheat (33), barley (33), Indian finger millet (34)	124–160	10	+	−	+	ND
γ-Purothionin type	Sorghum (35)	47–48	8	+	−	−	γ-Purothionins (36)
Ragi 1–2 type	Indian finger millet (37)	95	7	+	−	−	Phospholipid transfer proteins
Legume lectin type	Common beans (38)	246		+	+	−	Legume lectins (39)
Thaumatin type	Maize (40)	173–235	10–16	+	+	+	Pathogenesis-related protein (41), Osmotin (42), Thaumatin (43)
Knottin type	Amaranth (this work)	32	6	+	−	−	Proteinase inhibitors, neurotoxins (2)
Prokaryotic	Actinomycetes	75–120	4	+	+	−	ND

TABLE II
Amino acid sequences and inhibitor properties of the peptides used in this study

Peptide	Sequence (5 10 15 20 25 30)	Inhibition[a]	Folding ability[b]
AAI	**C**IPKWNR**C**GPK--MDGVP**CC**EPYT**C**TSDYYGN**C**S	+	+
nor6[c]	**C**IPKWUR**C**GPK--MDGVP**CC**EPYT**C**TSDYYGN**C**S	+	+
Δ3	**C**I-KWNR**C**GPK--MDGVP**CC**EPYT**C**TSDYYGN**C**S	−	+
Δ4	**C**IP-WNR**C**GPK--MDGVP**CC**EPYT**C**TSDYYGN**C**S	−	+
L6	**C**IPKWLR**C**GPK--MDGVP**CC**EPYT**C**TSDYYGN**C**S	+	+
IL5–6	**C**IPKILR**C**GPK--MDGVP**CC**EPYT**C**TSDYYGN**C**S	+	+
L7	**C**IPKWNL**C**GPK--MDGVP**CC**EPYT**C**TSDYYGN**C**S	−	+
Δ9	**C**IPKWNR**C**-PK--MDGVP**CC**EPYT**C**TSDYYGN**C**S	−	−
A10	**C**IPKWNR**C**GAK--MDGVP**CC**EPYT**C**TSDYYGN**C**S	+	−
A12	**C**IPKWNR**C**GPK--ADGVP**CC**EPYT**C**TSDYYGN**C**S	+	−
A14	**C**IPKWNR**C**GPK--MDAVP**CC**EPYT**C**TSDYYGN**C**S	+	−
A16	**C**IPKWNR**C**GPK--MDGVA**CC**EPYT**C**TSDYYGN**C**S	+	−
IL12–13	**C**IPKWNR**C**GPKILMDGVP**CC**EPYT**C**TSDYYGN**C**S	−	−
IL11–12	**C**IPKWNR**C**-PKILMDGVP**CC**EPYT**C**TSDYYGN**C**S	+	−
Chimera	A**C**IPKWNR**C**TPG----KNE**CC**PNRV**C**-SDKHKW**C**KWKL	See Table III	+
HWTX-I	A**C**KGVFDA**C**TPG----KNE**CC**PNRV**C**-SDKHKW**C**KWKL	See Table III	+

[a] Peptides exhibiting >1% inhibition at 15 μM concentration and 100:1 substrate/enzyme ratio were scored as "+."
[b] The folded products (Fig. 1) were purified by reverse phase-HPLC, and their quantity was estimated based on HPLC peak height (taking AAI as 100%). Cases where the quantity of the folded product reached 5% were scored as "+."
[c] U, norleucine.

columns for N-terminal sequencing carried out on a MilliGen/Biosearch model 6600 ProSequencer. The released amino acid phenylthiohydantoins were detected simultaneously at 269 and 313 nm.

Peptide Synthesis and Refolding Studies

AAI mutants (Table II) were synthesized manually by solid phase peptide synthesis methods based on FMOC chemistry and oxidative refolding as described (5). The Huwentoxin I chimera (Table II) was synthesized by FMOC chemistry on a PIONEER peptide synthesizer (PE Biosystems) using FMOC-L-Leu-polyethylene glycolpolystyrene resin as described (8). The oxidative refolding of the chimera was carried out in the presence of 0.1 mM oxidized glutathione and 1 mM reduced glutathione in 0.1 M acetate buffer, pH 9.5, containing 0.2 mM EDTA. The final product was purified by reverse phase-HPLC.

The qualitative ability of the peptides to fold was tested as follows. A stock solution of 1.0 mg of totally reduced and HPLC-purified peptide sample dissolved in 1 ml of freshly prepared argon-saturated refolding buffer (0.1 M NH_4Ac, 2 mM EDTA, 1 M guanidine hydrochloride, pH 7.8) was added to 49 ml of the same buffer to which 1 mM cysteine and 0.05 mM cystine were added immediately before use (the final concentration of the peptide was 20 μg/ml). After 16 h of stirring at 25 °C the reaction was stopped by adjusting the pH to 4.0 with acetic acid. The reaction mixture was analyzed by reverse phase-HPLC as described (5).The folding ability was evaluated from the chromatogram. Typical chromatograms of "well folding" (+) and "poorly folding" (−) samples are shown in Fig. 1,*A* and *B*, respectively. The peak corresponding to the folded product, indicated by the *arrow*, was collected and lyophilized for amylase inhibition assay.

NMR Studies

Sample Preparation—Samples were prepared by dissolving AAI powder in 0.5 ml of 20 mM phosphate or acetate buffer (90% H_2O, 10% D_2O) containing 0.02% NaN_3 and 0.1 mM EDTA with the final concentration of AAI being 2–4 mM. The pH of the solution was adjusted to 6.5 with 1N HCl and NaOH. Sodium 3-(trimethylsilyl)-2,2,3,3,-tetradeuteropropionate was added as an internal reference for chemical shifts to a final concentration of 200 μM. For the experiments in D_2O, AAI samples dissolved in H_2O were lyophilized and redissolved in 99.8% D_2O (Cambridge Isotope Laboratories). The solution was then allowed to stand at room temperature for 24 h before re-lyophilization and a second reconstitution with 99.996% D_2O.

NMR Spectroscopy—All of the two-dimensional spectra, including COSY, DQF-COSY, TOCSY, and NOESY, were collected at 500 MHz using a Bruker 500 AMX spectrometer at pH 6.5, 300 K. The data points were 512 in the F1 dimension and 2048 in the F2 dimension. Most two-dimensional spectra were recorded by the time proportional phase incrementation method (9). Solvent suppression was carried out by the presaturation method.

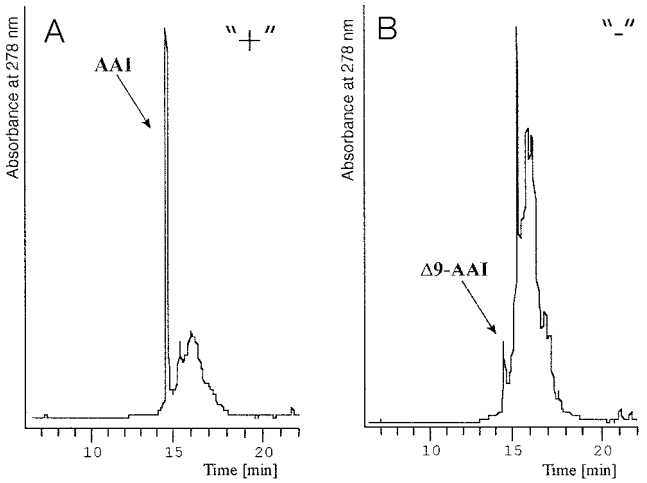

FIG. 1. **Chromatographic analysis of the folding ability of AAI analogs.** *A,* typical analytical reverse phase- HPLC tracing of a fully reduced synthetic AAI preparation after 16 h of refolding as indicated under "Experimental Procedures." *B,* HPLC tracing of a poorly folding peptide, Δ9-AAI (Table II) under the same conditions. Column, Supersphere 100 C_{18} 4 mm 4 × 125 column (Merck GmbH); buffer A, 0.1% trifluoroacetic acid in water; buffer B, 0.1% trifluoroacetic acid in acetonitrile; linear gradient from 15 to 40% buffer B in 25 min.

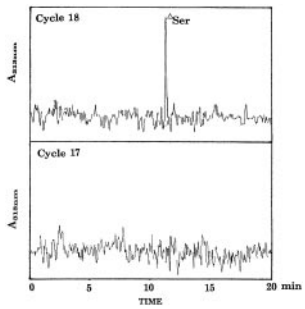

FIG. 2. **Identification of dehydroalanine (indicated as ΔSer) during Edman sequencing by monitoring the HPLC effluent at 313 nm.** Appearance of dehydroalanine in position 18 indicates only that this residue is disulfide-bonded to a sequentially upstream cystein, which, by way of elimination (see "Results"), is Cys^1.

Data Processing—SYBYL software (Tripos Inc.) was used on an Indigo 2 Silicon Graphics workstation. All the data were zero-filled to 1000 in the F1 dimension, resulting in a 2048 × 1024 (F2 × F1) real matrix. The sequential assignment method of Wüthrich (10) allowed identification of all backbone and side chain protons with the exception of a few side chain protons of Ile^2, Lys^4, Arg^7, Lys^{11}, and Glu^{19}. A total of 348 distance constraints were derived from the NOESY spectra (100 and 400 ms in H_2O and D_2O). 87 long distance constraints, 39 medium distance constraints, 101 sequential constraints, and 121 intraresidue constraints were found. Three distance constraints ($S(i) - S(j)$ (2.02 ± 0.02 Å), $S(i) - C_\beta(j)$ (2.99 ± 0.5 Å), and $S(j) - C_\beta(i)$ (2.99 ± 0.5 Å)) were used for each disulfide, and 8 dihedral constraints were calculated from one-dimensional spectrum and DQF-COSY. These constraints were used for calculating the structure with Brünger's X-PLOR, version 3.851 (11). The nuclear Overhauser effect spectroscopy constraints were divided into three classes (strong, medium, and weak), corresponding to the ranges of 1.8–2.8 Å, 1.8–3.5 Å, and 1.8–5.0 Å, respectively.

RESULTS

Structural Studies—Previous to the current study, the disulfide topology of AAI was only partially known, *i.e.* the connectivities of two vicinal Cys residues (17 and 18) were inferred from homology modeling rather than from experimental data. Because this is crucial to the NMR studies, we chose the Edman degradation method combined with phenylthiohydantoin analysis to confirm this disulfide topology at 313 nm. This combined method makes it possible to identify dehydroalanine, the β-elimination product of phenylthiohydantoin-cystine, which forms when the N-terminal sequencing process reaches a Cys residue disulfide bonded to a sequentially upstream Cys

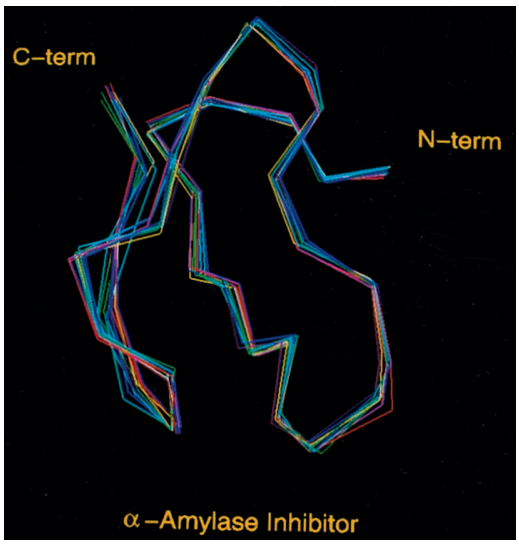

FIG. 3. **The C_α trace for the 10 best AAI structures obtained by NMR spectroscopy.** The C_α traces of the 10 best structures (*blue*) were superimposed, and the root mean square deviations were calculated using the molecular simulation program InsightII. The average root mean square distance was 0.32 Å for the backbone heavy atoms (N, C_α, C, and O) and 1.07 Å for all heavy atoms. N and C termini are indicated. The C_α trace of the final structure is shown in *red*.

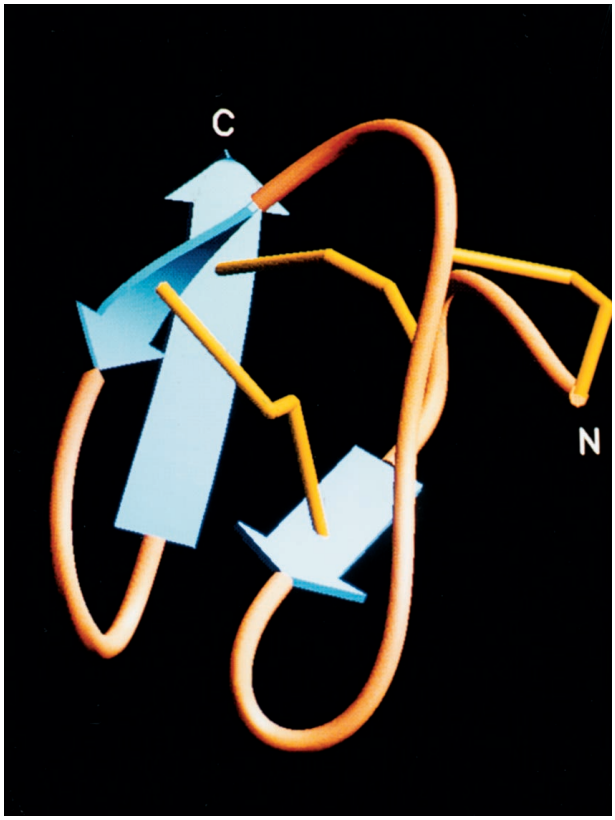

FIG. 4. **Ribbon diagram of the three-dimensional structure of AAI.** The best structure chosen from the results of PROCHECK (15) calculation is presented as a ribbon diagram produced with the program SETOR (44). The three β-strands, which form an antiparallel β-sheet are highlighted by *blue arrows,* and the three disulfide bridges are indicated in *yellow*. N and C termini are labeled.

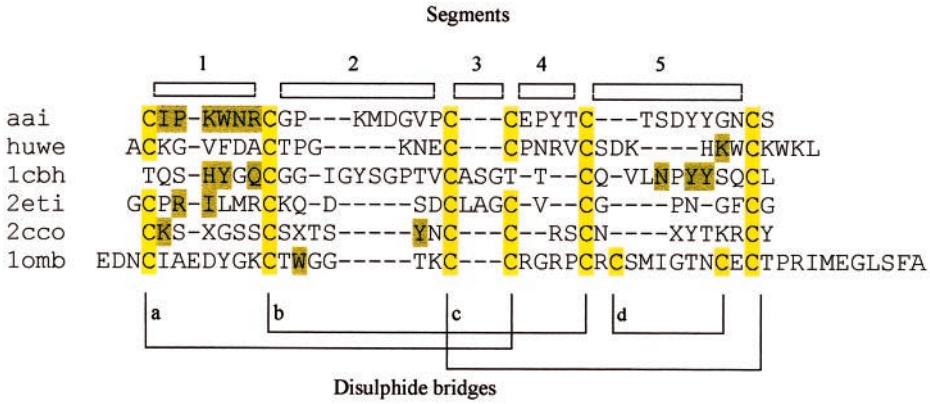

FIG. 5. **Structure-based alignment of selected knottin sequences.** *Dark yellow shading* indicates residues involved in ligand binding. AAI (*aai*) is from this study. Other proteins used are as follows: Huwentoxin-I, neurotoxin from the Chinese bird spider *Selenocosmia huwena* (*huwe*, Qu *et al.* (14); binding data, J. C. Luo, and X. Gu, unpublished results); the CB of the *T. reesei* cellobiohydrolase (PDB code, 1cbh; Kraulis *et al.* (45); binding data, Refs. 23–25); ω-conotoxin GVIA from the snail *Conus geographicus* (PDB code, 2cco; Davis *et al.* (46); binding data, Refs. 47–49); the trypsin inhibitor from *E. elaterium* (PDB code, 2eti; Chiche *et al.* (18); binding data, by homology from *C. maxima* inhibitor, Ref. 22); ω-agatoxin from the spider *Agelenopsis aperta* (PDB code, 1omb; Yun *et al.* (31); binding data, Ref. 28).

TABLE III
α-Amylase inhibition by a Huwentoxin I/AAI chimera

The sequences are shown in Table II. The α-amylase inhibitory activity was expressed as the difference between the two absorbance values obtained in the absence and in the presence of the peptide inhibitor (*i.e.* $(A)_{546\ control}$ $(A_{546\ peptide})$. The concentrations of α-amylase and inhibitor were adjusted so $A_{546\ nm}$ was in the optimal range.

Peptide substrate	Concentration	Molecular ratio of peptide to α-amylase	$(A)_{control}$-$(A)_{test}$	Inhibitory activity
	M			%
AAI	1.4×10^{-5}	0.14:1	0.060	100.00
Chimera	1.6×10^{-2}	260:1	0.076	0.07
Huwentoxin-I	1.1×10^{-1}	1100:1	0.000	0.00

residue (12). Fig. 2 clearly shows that the degradation product appears in position 18, confirming that AAI in fact has the disulfide topology Cys^1-Cys^{18}, Cys^8-Cys^{23}, Cys^{17}-Cys^{31}, a topological pattern characteristic of the knottin family.

50 structure calculations were carried out using the X-PLOR program of Brünger (11). The 10 best structures, based on their stereochemical energies (excluding the electrostatic term) and PROCHECK (15) results, were chosen for structure analysis. These structures (Fig. 3) had no nuclear Overhauser enhancement spectroscopy violations larger than 0.3 Å and no dihedral violations larger than 2 ° with 84.3% of all residues (excluding Gly and Pro) in the most favored regions and 15.7% in the additional allowed regions. A root mean square distance of 0.32 ± 0.05 Å was found for backbone atoms, whereas that for all heavy atoms was 1.04 ± 0.12 Å. Both values are satisfactorily low for a peptide of this size. These ten structures have been deposited in the Protein Structure Data Bank under the identification code "1qfd".

Using the protein structural element criteria described by Wüthrich (10), Richardson (16), and Wilmot and Thornton (17), we identified three antiparallel β-strands and five β-turns in the three-dimensional structure of AAI (Fig. 4). The three short β-strands include residues Arg^7-Cys^8, Thr^{22}-Thr^{24}, and Gly^{29}-Ser^{32}. The first strand is very short, a feature often prevalent in the knottin fold (4, 18). Of the five β-turns, Pro^3-Asn^6 belongs to type II, and Gly^9-Met^{12} and Pro^{10}-Asp^{13} belong to type I, whereas Glu^{19}-Thr^{22} and Asp^{26}-Gly^{29} belong to type VIII. Of the three disulfide bridges in this structure, Cys^1-Cys^{18} is a right-handed spiral, whereas Cys^8-Cys^{23} and Cys^{17}-Cys^{31} are left-handed.

Structure Comparison and Residue Replacement—The motif consists of three antiparallel β-strands accompanied by special disulfide bonding patterns and corresponds exactly to the so-called knottin (3) or inhibitor cystine knot fold (4). We therefore made a structural alignment for AAI with a set of known three-dimensional structures from this family (Fig. 5). In this figure we divided the sequences into segments between cysteine residues. To identify functionally and structurally important residues, we prepared a series of peptides carrying replacements or deletions in segment 1 or segment 2 and monitored, in a qualitative way, both their *in vitro* refolding ability (see "Experimental Procedures") as well as their α-amylase inhibitory activity (Table II). We found that although replacements in segment 2 impaired the folding ability of AAI, they did not abolish α-amylase activity. In contrast, replacements in segment 1 abolished α-amylase inhibition without drastic consequences for folding. To test whether segment 1 of AAI is directly involved in enzyme binding, we grafted it into Huwentoxin I, a protein, which although structurally similar to AAI, is not an α-amylase inhibitor. The resulting chimera (sequence shown in Table II) folded well (data not shown) and had a low but clearly significant α-amylase inhibitory activity (Table III). The inhibitory activity was 10^{-4} times that of AAI but very much higher than that of Huwentoxin I (inhibition was not detectable at the concentrations achievable with this peptide); because a successful scorpion toxin/charybdotoxin chimera had a bioactivity 10^{-5} that of the original charybdotoxin molecule (19), we infer that the inhibitory activity of our Huwentoxin I/AAI chimera construct is satisfactory proof that the segment 1 sequence is a part of the enzyme binding region of AAI.

DISCUSSION

The structure of AAI corresponds to the so-called knottin (3) or inhibitor cystine knot fold (4), which is characterized by three antiparallel β-strands and a disulfide topology of the "abcabc" type, as schematically shown in Fig. 5. The first of the

three β-strands is usually distorted, and it is missing in some members of this family so the core of this motif is often referred to as a short distorted triple-stranded β-sheet. In the solution structure of AAI the first β-strand is in fact less clearly defined than the other two. Members of this family do not show high sequence similarity, and, partly because of their small size, they cannot be easily identified by sequence similarity searches. We previously built a model of AAI based on its homology with the *Trichoderma reesei* CB and squash proteinase inhibitor (2). Although the global features of AAI were correctly captured by this model, the atomic coordinates were only in moderate agreement with the experimental data.

The knottin family contains several distinct subtypes, according to structure-based sequence alignment (Fig. 5). AAI, along with many of the fungal type CBs and some spider toxins, lacks segment 3, so these two central cysteines are vicinal. The CB of *T. reesei* cellobiohydrolase lacks the disulfide bridge *a*, whereas ω-conotoxin GVIA has an additional *d*. Huwentoxin I and other spider toxins form a distinct subgroup characterized by a very short third β-strand. AAI most closely resembles the fungal CB group.

The knottin (3) or inhibitor cystine knot fold (4) was found in various proteins from fungi, plants, spiders, and cone shells. The fact that these proteins fulfill a large variety of biological functions leads us to suggest that this fold may have emerged by convergent evolution. Thus the weak sequence similarities among various knottin proteins may be because of common structural determinants rather than a common evolutionary origin. In fact we have found that certain residues can be replaced without impairing the folding of the molecule, whereas other replacements seem to interfere with the folding. For example we found that segment 1 of AAI can accommodate residue replacements, which is in very good agreement with the finding that the *T. reesei* CB readily accepts mutations in the homologous region (20). It is interesting, in this respect, that formation of this simple fold is apparently not a one-step process. A two-step mechanism that includes the reshuffling of the first disulfide intermediates was suggested for AAI (5) and also for the related potato proteinase inhibitor (21). It is tempting to speculate that this suggested two-step mechanism may be in fact a condition for the formation of the knottin-structure; quantitative folding studies are now underway.

Members of the knottin family bind to various macromolecular ligands as diverse as cellular receptors, enzymes, or cellulose (for a recent overview see Ref. 20). In the structural alignment in Fig. 5 *green* displays the residues that are thought to be involved in binding. According to the distribution of these binding residues, knottins can be divided into three broad categories. The proteinase inhibitors from *Cucurbita maxima* (22) and *Ecballium elaterium* (18) bind through segment 1. The group, including the CB (23–25), charybdotoxin (26), and Huwentoxin I,[3] contains additional binding residues in segment 5. The third group, ω-conotoxin GVIA and ω-agatoxin interact via residues in segment 2 as well as segment 1. Our residue replacement results indicate that segment 1 of AAI seems to be involved in amylase binding but presumably is not solely responsible for it; however, the inhibition level of the chimera is low. Because our residue replacement studies failed to reveal binding residues in segment 2, which lead us to conclude that the binding mode of AAI may be different from that of ω-conotoxin GVIA and ω-agatoxin. So by elimination we are left with the conclusion that the binding mode of AAI may be similar to the *T. reesei* CB, *i.e.* the molecule may bind via segments 1 and 5. Conclusive data on the binding mode of AAI await analysis of the three-dimensional structure of an AAI/α-amylase complex.

Our AAI mutagenesis studies confirm that the knottin structure can accept a wide range of mutations. This is important for the engineering of small binding proteins with altered biological activities (20, 27). Finally, we note that the species-specific biological activity of AAI makes it an attractive target both for the development of insect-resistant transgenic plants (1), as well as in engineering studies (27).

Acknowledgments—We are grateful to Professors Yunyu Shi and Jihui Wu (University of Science and Technology, Hefei, China) for their invaluable help with NMR data collection, to Drs. Doriano Lamba, Alekos Athanasiadis, and Marie-Louise Tjörnhammar (ICGEB, Trieste) and Heather Smith-Xie (Peking University) for their advice regarding the manuscript.

Note Added in Proof—The three-dimensional structure of the complex of AAI with the *T. molitor* α amylase (PDB code:1clv) was recently determined by X-ray chrystallography (50).

[3] S. Liang and J. C. Luo, unpublished results.

REFERENCES

1. Ryan, C. A. (1989) *Bioessays* **10,** 20–24
2. Chagolla-Lopez, A., Blanco-Labra, A., Patthy, A., Sanchez, R., and Pongor, S. (1994) *J. Biol. Chem.* **269,** 23675–23680
3. Le-Nguyen, D., Heitz, A., Chiche, L., Castro, B., Boigegrain, R., Favel, A., and Coletti-Previero, M. (1990) *Biochimie* (*Paris*) **72,** 431–435
4. Pallaghy, P. K., Nielsen, K. J., Craik, D. J., and Norton, R. S. (1994) *Protein Sci.* **3,** 1833–1839
5. Lozanov, V., Guarnaccia, C., Patthy, A., Foti, S., and Pongor, S. (1997) *J. Pept. Res.* **50,** 65–72
6. Ohtsubo, K., and Richardson, M. (1992) *FEBS Lett.* **309,** 68–72
7. Bernfeld, P. (1955) *Methods Enzymol.* **1,** 149–158
8. Liang, S. P., Xia, Z. X., and Xie, J. Y. (1997) *Sci. China Ser. C Life Sci.* **40,** 449–457
9. Marion, D., and Wüthrich, K. (1983) *Biochem. Biophys. Res. Commun.* **13,** 967–974
10. Wüthrich, K. (1986) *NMR of Proteins and Nucleic Acids*, John Wiley & Sons, Inc., New York
11. Brünger, A. T. (1992) *X-PLOR Version 3.1: A System for X-ray Crystallography and NMR,* Yale University Press, New Haven, CT
12. Zhang, D., and Liang, S. (1993) *J. Protein Chem.* **12,** 735–740
13. Qu, Y., Liang, S., Ding, J., Ma, L., Zhang, R., and Gu, X. (1995) *J. Protein Chem.* **14,** 549–557
14. Qu, Y., Liang, S., Ding, J., Liu, X., Zhang, R., and Gu, X. (1997) *J. Protein Chem.* **16,** 565–574
15. Laskowski, R., MacArthur, M. W., Moss, F. S., and Thornton, J. M. (1993) *J. Appl. Crystallogr.* **26,** 283–291
16. Richardson, J. S. (1981) *Adv. Protein Chem.* **34,** 167–339
17. Wilmot., C. M., and Thornton, J. M. (1990) *Protein Eng.* **3,** 479–493
18. Chiche, L., Gaboriaud, C., Heitz, A., Mornon, J. P., Castro, B., and Kollmann, P. (1989) *Proteins* **6,** 405–414
19. Drakopoulou, E., Zinn-Justin, S., Guenneugues, M., Gilquin, B., Menez, A., and Vita, C. (1996) *J. Biol. Chem.* **271,** 11979–11987
20. Smith, G. P., Patel, S. U., Windass, J. D., Thornton, J. M., Winter, G., and Griffiths, A. D. (1998) *J. Mol. Biol.* **277,** 317–332
21. Chang, J. Y., Canals, F., Schindler, P., Querol, E., and Aviles, F. X. (1994) *J. Biol. Chem.* **269,** 22087–22094
22. Bode, W., Geyerling, H. J., Huber, R., Otlewski, J., and Wilusz, T. (1989) *FEBS Lett.* **242,** 285–292
23. Reinikainen, T., Teleman, O., and Teeri, T. T. (1995) *Proteins* **22,** 392–403
24. Reinikainen, T., Ruohonen, L., Nevanen, T., Laaksonen, L., Kraulis, P., Jones, T. A., Knowles, J. K., and Teeri, T. T. (1992) *Proteins* **14,** 475–482
25. Linder, M., Mattinen, M. L., Kontteli, M., Lindeberg, G., Stahlberg, J., Drakenberg, T., Reinikainen, T., Pettersson, G., and Annila, A. (1995) *Protein Sci.* **4,** 1056–1064
26. Park, C. S., and Miller, C. (1992) *Biochemistry* **31,** 7749–7755
27. Vita, C., Vizzavona, J., Drakopoulou, E., Zinn-Justin, S., Gilquin, B., and Menez, A. (1998) *Biopolymers* **47,** 93–100
28. Nishiuchi, Y., Kumagaye, K., Noda, Y., Watanabe, T. X., and Sakakibara, S. (1986) *Biopolymers* **25,** S61–S68
29. Svendsen, M. J., Hejgaard, J., and Mundy, J. (1986) *Carlsberg Res. Commun.* **51,** 493–500
30. Maeda, K. (1986) *Biochim. Biophys. Acta* **871,** 250–256
31. Yu, H., Rosen, M. K., Saccomano, N. A., Phillips, D., Volkmann, R. A., and Schreiber, S. L. (1993) *Biochemistry* **32,** 13123–13129
32. Kurihara, Y. (1992) *Crit. Rev. Food Sci. Nutr.* **32,** 231–252
33. Richardson, M. (1990) in *Methods in Plant Biochemistry* (Rogers, L., ed) Vol. 5, pp. 261–307, Academic Press, London
34. Campos, F. A. P., and Richardson, M. (1983) *FEBS Lett.* **152,** 300–304
35. Bloch, C., Jr., and Richardson, M. (1991) *FEBS Lett.* **279,** 101–104
36. Olmedo, F. G., and Palenzuela, P. R. (1989) *Oxf. Surv. Plant. Mol. Cell. Biol.* **6,** 31–60
37. Campos, F. A. P., and Richardson, M. (1984) *FEBS Lett.* **167,** 221–225
38. Moreno, J., and Chrispeels, M. J. (1989) *Proc. Natl. Acad. Sci. U. S. A.* **86,** 7885–7889
39. Lis, H., and Sharon, N. (1986) *Annu. Rev. Biochem.* **55,** 33–37
40. Richardson, M., Valdez-Rodriguez, S., and Blanco-Labra, A. (1987) *Nature* **327,** 432–434

41. Pierpoint, W. S., Tatham, A. S., and Pappin, D. J. C. (1987) *Physiol. Mol. Plant Pathol.* **31,** 291–298
42. Singh, N. K., Nelson, D. E., Kuhn, D., Hasegawa, P. M., and Bressan, R. A. (1989) *Plant Physiol.* (*Bethesda*) **90,** 1096–1101
43. Ivengar, R. B., Sits, P., Ouderaa, F. V. d., WEL, H. V. d., Brouvershaaven, J. V., Ravenstein, P., Richters, G., and Wassenaar, P. D. V. (1979) *Eur. J. Biochem.* **96,** 193–204
44. Evans, S. V. (1993) *J. Mol. Graph.* **11,** 134–138
45. Kraulis, J., Clore, G. M., Nilges, M., Jones, T. A., Pettersson, G., Knowles, J., and Gronenborn, A. M. (1989) *Biochemistry* **28,** 7241–7257
46. Davis, J. H., Bradley, E. K., and Basus, V. J. (1993) *Biochemistry* **32,** 7396–7405
47. Lampe, R. A., Lo, M. M., Keith, R. A., Horn, M. B., McLane, M. W., Herman, J. L., and Spreen, R. C. (1993) *Biochemistry* **32,** 3255–3260
48. Sato, K., Park, N. G., Kohno, T., Maeda, T., Kim, J. I., Kato, R., and Takahashi, M. (1993) *Biochem. Biophys. Res. Commun.* **194,** 1292–1296
49. Kim, J. I., Takahashi, M., Ogura, A., Kohno, T., Kudo, Y., and Sato, K. (1994) *J. Biol. Chem.* **269,** 23876–23878
50. Pereira Barbosa, P. J. B., Lozanov, V., Patthy, A., Huber, R., Bode, W., Pongor, S., and Strobl, S. (1999) *Structure*, in press